Supplement of Clim. Past, 22, 1023–1036, 2026
https://doi.org/10.5194/cp-22-1023-2026-supplement

Supplement of

Microscale alkenone heterogeneity and replicability of ultra-high-resolution temperature records from marine sediments

Jannis Viola et al.

Correspondence to: Jannis Viola (jannis.viola@awi.de)

S1 FT ICR MS settings

Table S1: Selected parameters for laser-desorption-ionization (LDI) FT-ICR-MS for compounds in the mass range around 554 m/z ("alkenone window")

Setting	**Value**
Q1 (m/z)	554 m/z
Q1range (m/z)	544-564
wordsize	512k
Detection mode	broadband
excitation mode	sweep
excitation range (m/z)	300-2000
shotraster	100µm
scans per shot	1
spot size	medium
laser power	varied according to sediment conditions
laser frequency	500 Hz
laser number of shots	250
Plate 1 final voltage for ramp 2	0.0 V
Plate 1 initial ramp voltage	1.0 V
Plate 1 final voltage for ramp 1	0.6 V
Gated Injection DC Bias 0	3.6 V
Internal Filament Current [Instrument Param]	0.500 A
Plate 2 initial ramp voltage	1.0 V
Plate 2 final voltage for ramp 1	0.6 V
Plate 2 final voltage for ramp 2	0.0 V
Gated Injection DC Bias 180	2.4 V
Front Trap Plate	3.0 V
Back Trap Plate	3.0 V
Internal Ionization Energy	1.0 eV
Gated Injection DC Bias 90	2.7 V
Back Trap Plate Quench	-30.0 V
Sidekick	0.0 V

Shimming DC Bias 90	3.0 V
Shimming DC Bias 270	3.0 V
Shimming DC Bias 0	3.0 V
Shimming DC Bias 180	3.0 V
ECD Lens	10.0 V
Gated Injection DC Bias 270	3.3 V
Analyzer Entrance	-10.0 V
Sidekick Offset	-1.5 V
Octopole 2 DC [Instrument Param]	2.0 V
Octopole Frequency	1
Extract [Instrument Param]	-10.0 V
Trap [Instrument Param]	10.0 V
Octopole 1 DC Bias (Low) [Instrument Param]	3.5 V
Octopole 2 DC Bias (High)	2.5 V
Octopole RF Amplitude	350.0 Vpp
Partition Lens [Instrument Param]	3.0 V
Octopole 2 Delta DC	0.0 V

After the measurements, the data was lockmass calibrated using Bruker Compass DataAnalysis 5.0 SR1 (Bruker Daltonik Gmbh, 2017). Lockmass target was the Na^+ adduct of pyropheophorbide α ($C_{33}H_{34}N_4O_3Na$, 557.2523 m/z). Peak intensities and SNR_{FT} were exported for C37:2, C37:3 and pyropheophorbide α and filtered with $SNR_{FT} \geq 5$ prior further use. It is important to note that SNR_{FT} is a relative metric and depends on peak intensities in the surrounding m/z range, as well as measurement and processing parameters, so that the values or thresholds are not comparable between studies and different settings.

S2 Age control & stratigraphic alignment of MV1012-001KC ("KC1")

Figure S1 (right): X-ray scans of LL-channel sediment "slab" samples of MV1012-001KC on left to right: "KC1B" (named KC1 in this study), "KC1A" (sample from same core, ~5 cm apart, not used) and MV0811-14TC, used by Liu et al. (in prep). Direction is core top at the top of the image, downcore direction is down. The sediment section "KC1" of this study is visible in the bottom left corner.

Brighter values in the X-ray image correspond to denser sediment. White triangle markers are for keeping orientation of the samples during X-ray imaging; pointing towards the top of the sediment. Black holes are markers for keeping orientation of the 5 cm pieces during sample handling and processing.

We identify event layers or marker horizons after Hendy et al. (2013) and follow their naming scheme. We additionally compared to core photos and flood stratigraphies of Du et al. (2018).

Dashed yellow lines indicate grey flood layers which we identify as event 1A (1861 AD) and 1C (1761 AD). The upper green dotted line corresponds to the 1B olive bioturbated (Macoma (Schimmelmann et al., 1992)) layer (1841 AD), note the burrow or movement disturbance throughout K1C1 00-30 cm. The lower green dotted line corresponds to olive turbidite 1D (1738 AD). KC1A 30-60 potentially additionally contains event 1E another grey flood layer (1532 AD).

The distances from KC1 to SPR0901-02KC & 06KC used by Hendy et al. (2013) are ~ 0.85 km & ~ 2.1 km; from KC1 to MV0811-14TC used by Liu et al. (in prep) and Du et al. (2018) ~ 0.14 km.

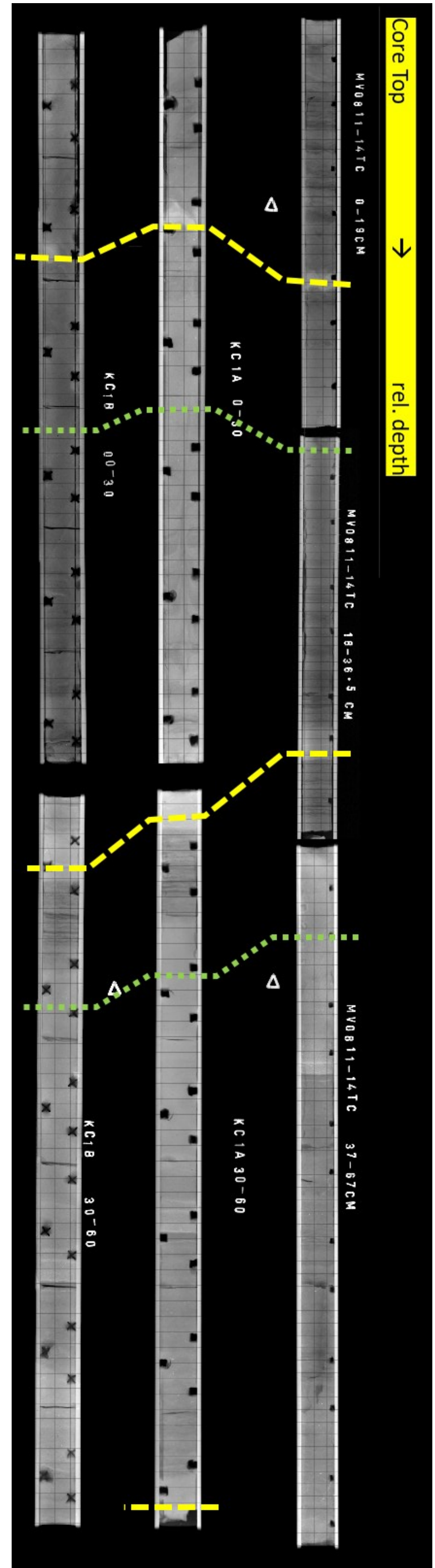

S3 Correlation and SNR

As SNR quantifies the amount of *any* shared variation between replicates, which can be based on a combination of correlated noise and shared climatic signal, we can convert SNR to an estimate of an expected upper bound of achievable correlation of an individual timeseries to the true climate signal:

$$r_{max} = \sqrt{\frac{SNR}{1 + SNR}}$$

.

S4 Xray Image Correction

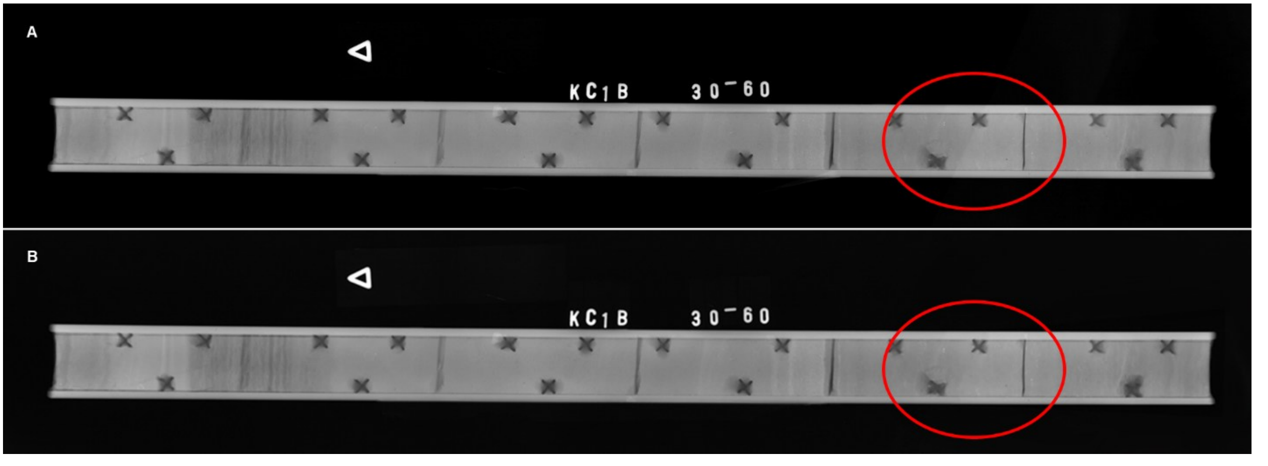

Figure S2: Comparison of the unaltered and corrected X-ray density maps for sediment segment KC1. Section 20-25 cm had an exposure artefact after developing. We thank A. Breuer (a.breuer@fu-berlin.de) for the digital corrections made using Adobe Photoshop (2024).

S5 Time series summary

Table S2: Time-series data and row-wise averages across replicates per depth interval. Standard errors below 0.001 (~0.03°C) are not shown.

Depth (cm)	Mean	Variance	Average variance of swUK per horizon	Average number of successful detections of both alkenones per horizon	Average number of successful detections of any alkenone per horizon
0-5	0.523	0.00044	0.006	34.2 ± 1.6	38.6 ± 1.8
5-10	0.536 ± 0.001	0.000412	0.0059	42.2 ± 0.8	48.1 ± 0.9
10-15	0.543	0.000611	0.006	16 ± 0.8	19.2 ± 0.9
15-20	0.539 ± 0.001	0.000388	0.0062	24.8 ± 1	31.4 ± 1.1
20-25	0.538 ± 0.001	0.000898	0.0061	32.2 ± 3.8	38.4 ± 4.4
25-30	0.530 ± 0.001	0.000994	0.0059	39 ± 1.9	46.3 ± 1.7

S6 Individual variograms per depth

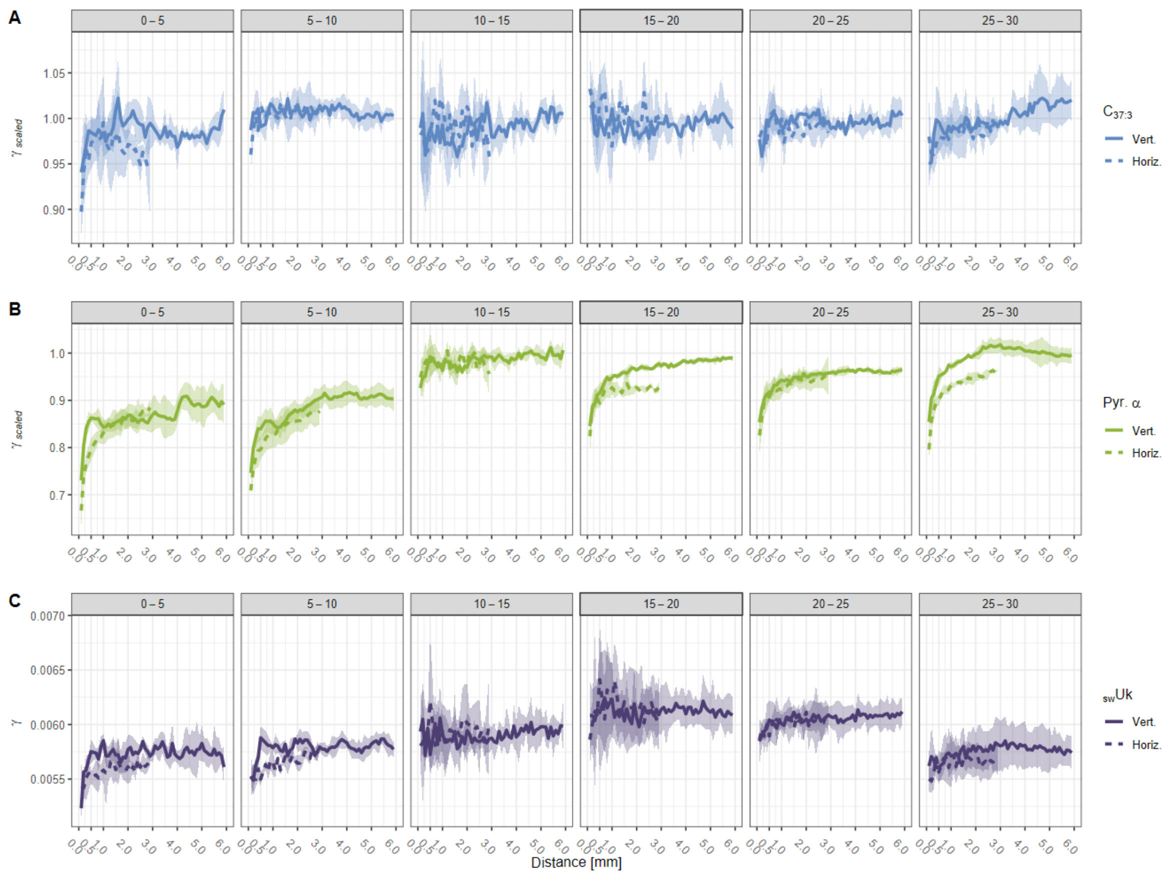

Figure S3: Variogram estimates averaged per depth interval of sediment segment KC1 for C37:3 and pyropheophorbide α intensities and spotwise Uk'37 temperatures. Note that each row has individual y-axes. C37:3 and pyropheophorbide α values in A, B were scaled prior calculation and are not in their native units, whereas in C γ values correspond to spotwise $U_{37}^{K'}$ units. Solid lines ("vertical") indicate estimates along the downcore direction, dotted lines indicate estimates along horizons, i.e. lateral, approximately parallel to lamina and the sediment surface (each within 10° tolerance angles).

S7 Comparison to SST

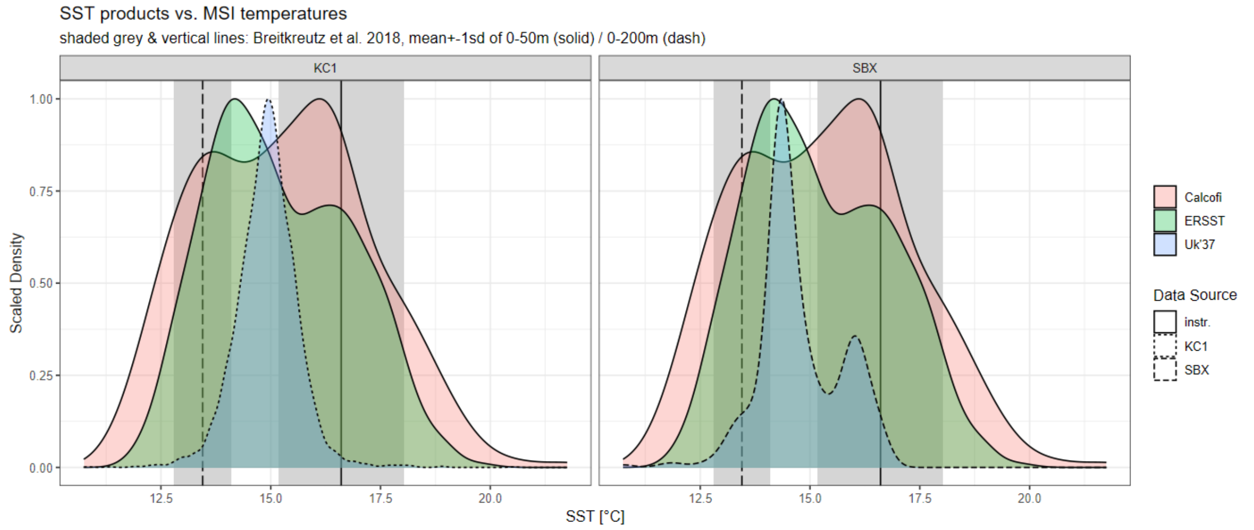

Figure S4: Comparison of MSI-derived SST estimates and SST products. Sediment data from KC1 segment, and the SBX 20-25cm exemplary varved section from Alfken et al. 2020, both converted to temperature using ISU and MSW approaches and the Prahl & Wakeham (1987) calibration ($U^{K'}_{37} = 0.033T + 0.043$). External SST data from the nearest location in Breitkreutz et al. (2018) (Lon: -119.5, Lat: 33.5) shown as vertical lines and shaded grey area (mean+-1sd of 0-50m and 0-200m respectively); ERSSTv4 (Huang et al., 2015) at Lon: 120, Lat: 34); and the nearest CalCOFI station (81.8-46.9) temperatures integrated 0-30m over 1984-2009 (California State Department of Fish and Game; NOAA Fisheries; Scripps Institution of Oceanography, 2001) (accessed 03/03/2023).

References

Adobe Inc., 2024. Adobe Photoshop (Version 2024). San Jose, CA: Adobe Systems Incorporated.

Alfken, S., Wörmer, L., Lipp, J.S., Wendt, J., Schimmelmann, A., Hinrichs, K., 2020. Mechanistic Insights Into Molecular Proxies Through Comparison of Subannually Resolved Sedimentary Records With Instrumental Water Column Data in the Santa Barbara Basin, Southern California. Paleoceanography and Paleoclimatology 35. https://doi.org/10.1029/2020PA004076

Breitkreuz, C., Paul, A., Kurahashi-Nakamura, T., Losch, M., Schulz, M., 2018. A Dynamical Reconstruction of the Global Monthly Mean Oxygen Isotopic Composition of Seawater. Journal of Geophysical Research: Oceans 123, 7206–7219. https://doi.org/10.1029/2018JC014300

California State Department of Fish and Game; NOAA Fisheries; Scripps Institution of Oceanography, 2001. Chemical, physical, and other data collected in the coastal waters of California as part of the California Cooperative Fisheries Investigation (CalCOFI) project since 1949.

Prahl, F.G., Wakeham, S.G., 1987. Calibration of unsaturation patterns in long-chain ketone compositions for palaeotemperature assessment. Nature 330, 367–369. https://doi.org/10.1038/330367a0

Huang, B., Banzon, V.F., Freeman, E., Lawrimore, J., Liu, W., Peterson, T.C., Smith, T.M., Thorne, P.W., Woodruff, S.D., Zhang, H.-M., 2015. Extended Reconstructed Sea Surface Temperature Version 4 (ERSST.v4). Part I: Upgrades and Intercomparisons. Journal of Climate 28, 911–930. https://doi.org/10.1175/JCLI-D-14-00006.1